Proceedings of the 43rd "Jaszowiec", International School and Conference on the Physics of Semiconductors, Wisła 2014

Magnetic Order and Magnetic Inhomogeneities in SnCrTe–PbCrTe Solid Solutions

L. Kilanski[a,*], M. Szymański[a,b], B. Brodowska[a], M. Górska[a], R. Szymczak[a], A. Podgórni[a], A. Avdonin[a], A. Reszka[a], B.J. Kowalski[a], V. Domukhovski[a], M. Arciszewska[a], W. Dobrowolski[a], V.E. Slynko[c] and E.I. Slynko[c]

[a]Institute of Physics, Polish Academy of Sciences, al. Lotników 32/46, 02-668 Warszawa, Poland

[b]Faculty of Materials Engineering, Warsaw University of Technology, Wołoska 141, 02-507 Warszawa, Poland

[c]Institute of Materials Science Problems, Ukrainian Academy of Sciences, 5 Wilde Str., 274001 Chernovtsy, Ukraine

We present the studies of structural, electrical and magnetic properties of bulk $Sn_{1-x-y}Pb_xCr_yTe$ mixed crystals with chemical composition $0.18 \leq x \leq 0.35$ and $0.007 \leq y \leq 0.071$. The magnetometric studies indicate that for the high Cr-content, $y = 0.071$, the alloy shows ferromagnetic alignment with the Curie temperature, T_C, around 265 K. The Cr_5Te_8 clusters are responsible for the ferromagnetic order. At low Cr content, $y \approx 0.01$, a peak in the ac magnetic susceptibility identified as the cluster-glass-like transition is observed at a temperature about 130 K. The cluster-glass-like transition is likely due to the presence of Cr_2Te_3 clusters in the samples with $y \approx 0.01$. The transport characterization of the samples indicated strong metallic p-type conductivity with relatively high carrier concentration, $n > 10^{20}$ cm^{-3}, and carrier mobility, $\mu > 150$ cm^2/(V s).

DOI: 10.12693/APhysPolA.126.1203

PACS: 72.80.Ga, 75.30.Hx, 75.30.Et, 75.50.Pp

1. Introduction

Semimagnetic semiconductors based on transition metal doped IV–VI materials are of particular interest due to the presence of carrier mediated ferromagnetism with Curie temperature, T_C, as high as 200 K for $Ge_{1-x}Mn_xTe$ with $x = 0.5$ [1]. Chromium alloyed IV–VI materials such as GeTe also show ferromagnetism with transition temperatures as high as 160 K for thin layers [2] and 60 K for bulk crystals [3–5]. Other IV–VI materials are also of large interest in the field of possible applications in spintronics. Eggenkamp et al. investigated magnetic properties of $Sn_{1-x}Mn_xTe$ and showed ferromagnetism with critical temperatures changing from 3 K up to 16 K for Mn-content, x, changing from 0.03 to 0.1, respectively [6]. Chromium alloying of SnTe caused a presence of clusters with a high content of chromium, around $x = 0.25$, and the bulk matrix with randomly distributed Cr ions having the concentration equal to about 20% of the average composition x [7]. In the present paper we investigate the problem of alloying the SnTe–PbTe solid solutions with Cr ions. Our main goal was to see whether SnTe–PbTe solid solution can improve chromium solubility with respect to SnTe. We would like to explore the main exchange mechanisms present in the $Sn_{1-x-y}Pb_xCr_yTe$ alloy.

2. Experimental

Bulk $Sn_{1-x-y}Pb_xCr_yTe$ crystals were synthesized with the use of a modified Bridgman method. The modifications of the growth procedure were similar to those employed by Aust and Chalmers for the growth of alumina crystals [8]. The as-grown crystals were cut into 1 mm thick slices perpendicular to the growth direction. The chemical composition of our crystals was characterized with the use of an energy dispersive X-ray fluorescence (EDXRF) spectrometer. This method allows the determination of chemical composition of the alloy with maximum relative errors in the molar fraction of alloying elements, x and y, not exceeding 10% of the estimated value. The results indicate that the chemical content of $Sn_{1-x-y}Pb_xCr_yTe$ slices changes along the ingot length with x changing continuously from 0.17 to 0.35, and y from roughly 0.01 in most of our samples up to about 0.07. From all the slices we selected a few for further studies.

3. Results

The structural quality of our samples was studied by means of standard X-ray powder diffraction (XRD) technique using Siemens D5000 diffractometer at room temperature. Exemplary diffraction patterns for two different samples with different chemical compositions are presented in Fig. 1. The XRD results were analyzed with the use of the Rietveld refinement method. The diffraction patterns observed for the samples with low Cr-content, $y \approx 0.01$, show features characteristic of a SnTe phase only. The addition of Pb to the alloy does not lower its structural quality. The increase of Cr-content in the alloy ($y \approx 0.07$) leads to appearance of additional diffraction patterns, which could not be directly assigned to any known Sn-Pb-Cr-Te phases. The lattice parameter a, calculated using the Rietveld method (see the inset to Fig. 1) is close to the value for SnTe crystals, i.e., $a = 6.327$ Å [9].

*corresponding author; e-mail: lukasz.kilanski@ifpan.edu.pl

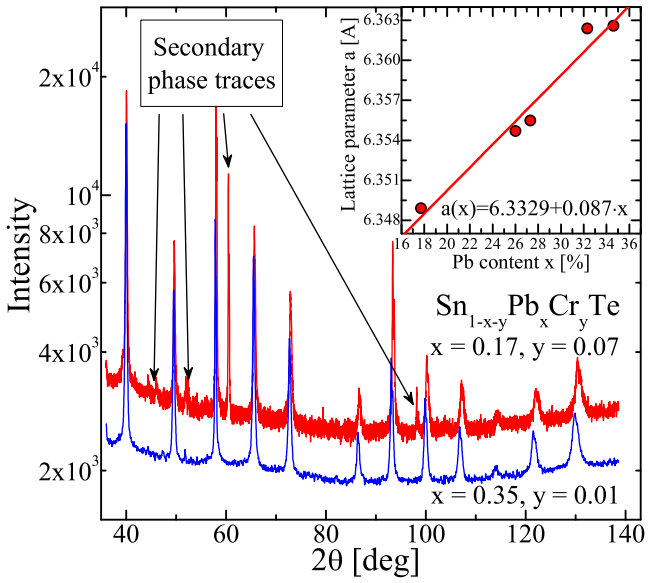

Fig. 1. Exemplary diffraction patterns obtained for the selected $Sn_{1-x-y}Pb_xCr_yTe$ crystals with different chemical composition. The inset shows the lattice parameter a as a function of the Pb content, x.

The $a(x)$ changes according to the Vegard law (see the inset to Fig. 1). It is a signature that the synthesis of the SnTe–PbTe alloy was successful.

Hitachi SU-70 Analytical ultra high resolution field emission scanning electron microscope (SEM) coupled with Thermo Scientific NSS 312 energy dispersive X-ray spectrometer (EDS) equipped with silicon drift detector was used in order to study the chemical homogeneity of our $Sn_{1-x}Cr_xTe$ samples. A series of SEM images and EDS maps were measured in order to identify the second phase observed during XRD studies. Exemplary SEM/EDS results are presented in Fig. 2. These maps show the presence of mostly Cr and Te ions in the clusters. The chemical composition measurements done with the use of a EDS microprobe reveal that the stoichiometry ratio of Cr to Te ions is similar in the samples with $y \approx 0.01$ and 0.07 and varies from 59% to 69%. That indicates possible Cr_2Te_3 or Cr_5Te_8 clusters.

The electrical transport of the $Sn_{1-x-y}Pb_xCr_yTe$ crystals was studied with the use of a standard dc current six contact Hall effect technique in a magnetic field $B = 1.5$ T and at temperatures from 4.3 K up to 300 K. The results indicate that all our samples are p-type semiconductors with high carrier concentration, $p \approx 10^{20}$ cm^{-3}, and relatively low carrier mobility, $\mu < 700$ cm^2/(V s). The metallic resistivity vs. temperature relation, $\rho_{xx}(T)$ typical of degenerated semiconductor, is observed. The Hall carrier concentration does not show changes with the temperature. The $\mu(T)$ dependence for all our samples does show a decrease of μ with increasing T, a feature typical of the reduction of the mobility due to phonon scattering.

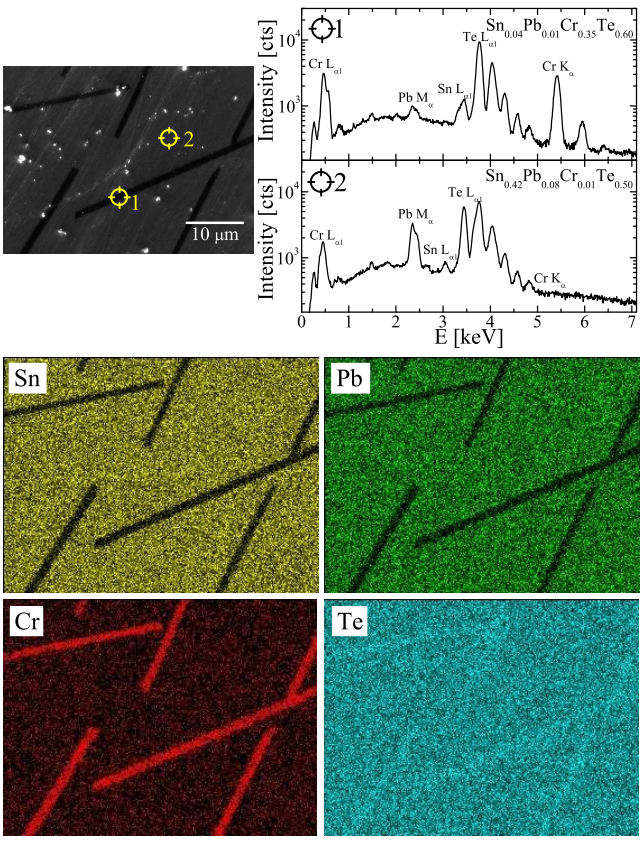

Fig. 2. Results of the SEM/EDS measurements including: SEM image with EDS spectra measured at selected points followed by EDS maps showing the distribution of alloying elements.

Magnetic properties of our $Sn_{1-x-y}Cr_xEu_yTe$ samples were studied with the use of dynamic susceptibility and static magnetization measurement techniques with the use of LakeShore 7229 susceptometer/magnetometer system. The temperature dependence of the ac magnetic susceptibility, χ_{ac}, was measured over the broad temperature range from 4.3 K up to 300 K. During the measurements the sample was placed in an alternating magnetic field with frequency f equal to 625 Hz and amplitude $B_{ac} = 1$ mT. The temperature dependence of the real part of the ac magnetic susceptibility, $\mathrm{Re}(\chi_{ac})(T)$, for a few selected $Sn_{1-x-y}Pb_xCr_yTe$ crystals is presented in Fig. 3. The results indicate a completely different behavior of the samples with Cr content around $y = 0.01$ and 0.07. The magnetic susceptibility for the sample with $y = 0.07$ has values more than an order of magnitude higher than for $y = 0.01$. The temperature dependence of the magnetic susceptibility for the samples with $y = 0.07$ shows a paramagnet–ferromagnet transition located at temperatures close to 300 K. The Curie temperature, determined from the inverse of the magnetic susceptibility has a value of about 266 ± 10 K. The ferromagnetic alignment of Cr-ions in this sample is related to the presence of Cr-Te clusters detected with

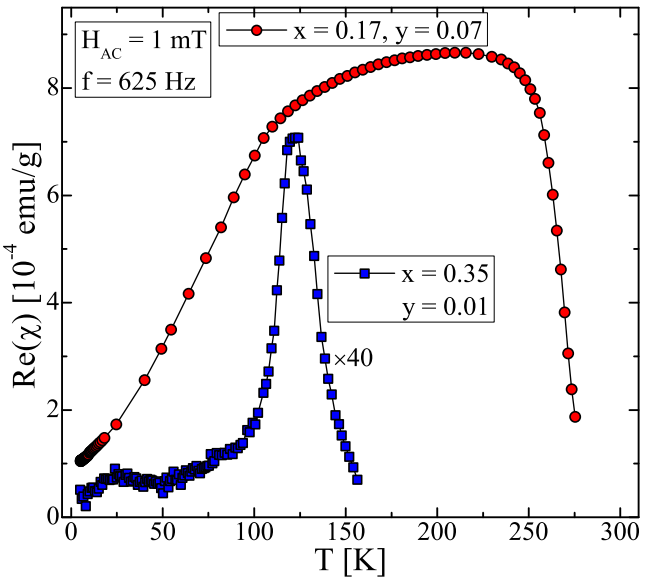

Fig. 3. The temperature dependence of the ac magnetic susceptibility for the selected $Sn_{1-x-y}Pb_xCr_yTe$ samples with different chemical content, x and y.

SEM/EDS technique. Cr_5Te_8, Cr_2Te_3, and $CrTe_2$ phases show the Curie temperature of about 190–245 K [10], 170 K [11] and 18 K [12], respectively. The other known phases are CrTe [13], Cr_7Te_8 [14, 15], Cr_5Te_6 [15], and Cr_3Te_4 [15, 16] with the Curie temperatures well above 300 K. The literature data show that the most probable Cr–Te-related clusters that could be responsible for the ferromagnetic order in this sample are Cr_5Te_8 clusters. The difference between the T_C observed for our samples (266 K) and the values reported for Cr_5Te_8 (190–245 K) may be due to the fact that the ferromagnetic clusters are placed in diamagnetic Sn-Pb-Te matrix. Furthermore, in the present study the clusters may not have proper stoichiometry; that may cause changes in the Curie temperature. Below approximately 120 K the magnetic susceptibility decreases with temperature. This behavior is incomprehensible. A ferromagnet should maintain a high value of the magnetic susceptibility over the entire temperature range below the Curie temperature. The reduction of the magnetic susceptibility below 120 K indicates the possibility of occurrence of a cluster-glass state at low temperature.

The magnetic susceptibility for the $Sn_{1-x-y}Pb_xCr_yTe$ samples with $y \approx 0.01$ shows the presence of a well defined peak at temperatures around 120–140 K. In order to determine the type of the observed magnetic state the detailed measurements of the $\mathrm{Re}(\chi_{ac})(T)$ dependence with the use of an alternating magnetic field of different frequency f in the range from 7 Hz to 9980 Hz were performed. The $\mathrm{Re}(\chi_{ac})(T)$ dependence shifted towards higher temperatures with increasing f, in a way similar as for the $Ge_{1-x-y}Sn_xMn_yTe$ (Refs. [17–19]), $Ge_{1-x-y}Cr_xEu_yTe$ (Refs. [4, 5]), and $Ge_{1-x-y}Mn_xEu_yTe$ crystals (Ref. [20]). That effect was identified as the appearance of a cluster-spin-glass freezing of the Cr_2Te_3 grains.

The measurements of magnetization vs. magnetic field, $M(B)$, were performed up to $B = 9$ T. We used the Weiss extraction method included in the LakeShore 7229 magnetometer system. Isothermal magnetic hysteresis loops were measured at selected temperatures, $T < 200$ K. Exemplary $M(B)$ curves obtained for the selected $Sn_{1-x-y}Pb_xCr_yTe$ crystals are presented in Fig. 4. The results indicate that in case of the samples with $y \approx 0.01$ the magnetization is much lower than would follow from the difference in composition only. The Brillouin-like shape of the $M(B)$ curve and a narrow hysteresis loop is observed for the sample with $y \approx 0.07$, a feature typical of the ferromagnetic material.

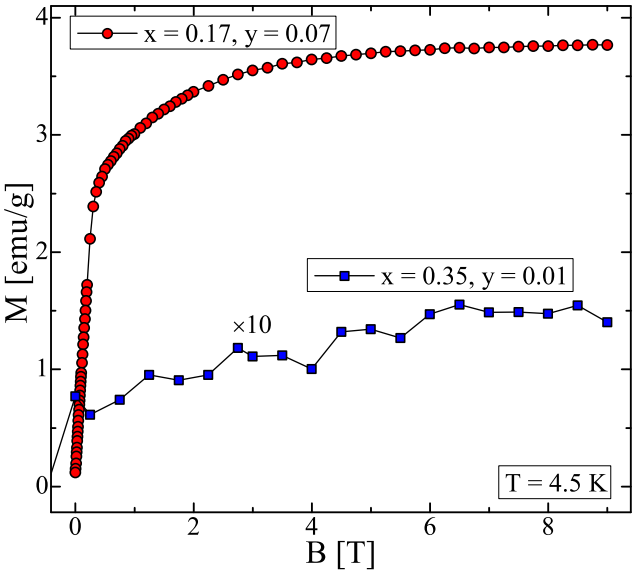

Fig. 4. Exemplary magnetic field dependences of the magnetization obtained for the selected $Sn_{1-x-y}Pb_xCr_yTe$ crystals with different chemical composition, x and y, obtained at $T = 4.5$ K.

4. Conclusions

The presence of Cr_2Te_3 and Cr_5Te_8 clusters is responsible for the magnetic properties of the $Sn_{1-x-y}Pb_xCr_yTe$ crystals with $y \approx 0.01$ and $y \approx 0.07$, respectively. The SnTe–PbTe solid solution synthesis is successful but it does not improve the solubility of Cr in IV–VI matrix. On the contrary to $Sn_{1-x}Cr_xTe$ alloy the $Sn_{1-x-y}Pb_xCr_yTe$ crystal synthesis produces clusters of typical Cr–Te compounds rather than clusters of the IV–VI host materials with high content of Cr.

Acknowledgments

The research was supported by the Foundation for Polish Science — Homing-Plus Programme co-financed by the European Union within European Regional Development Fund.

References

[1] R.T. Lechner, G. Springholz, M. Hassan, H. Groiss, R. Kirchschlager, J. Stangl, N. Hrauda, G. Bauer, *Appl. Phys. Lett.* **97**, 023101 (2010).

[2] Y. Fukuma, H. Asada, N. Moritake, T. Irisa, T. Koyanagi, *Appl. Phys. Lett.* **91**, 092501 (2007).

[3] L. Kilanski, M. Górska, W. Dobrowolski, M. Arciszewska, V. Domukhovski, J.R. Anderson, N.P. Butch, A. Podgórni, V.E. Slynko, E.I. Slynko, *Acta Phys. Pol. A* **119**, 654 (2011).

[4] L. Kilanski, A. Podgórni, W. Dobrowolski, M. Górska, B.J. Kowalski, A. Reszka, V. Domukhovski, A. Szczerbakow, K. Szałowski, J.R. Anderson, N.P. Butch, V.E. Slynko, E.I. Slynko, *J. Appl. Phys.* **112**, 123909 (2012).

[5] A. Podgórni, L. Kilanski, W. Dobrowolski, M. Górska, A. Reszka, V. Domukhovski, B.J. Kowalski, J.R. Anderson, N.P. Butch, V.E. Slynko, E.I. Slynko, *Acta Phys. Pol. A* **122**, 1012 (2012).

[6] P.J.T. Eggenkamp, C.W.H.M. Vennix, T. Story, H.J.M. Swagten, C.H.W. Swüste, W.J.M. de Jonge, *J. Appl. Phys.* **75**, 5728 (1994).

[7] L. Kilanski, A. Podgórni, M. Górska, W. Dobrowolski, V.E. Slynko, E.I. Slynko, *Acta Phys. Pol. A* **124**, 881 (2013).

[8] K.T. Aust, B. Chalmers, *Can. J. Phys.* **36**, 977 (1958).

[9] G. Nimtz, B. Schlicht, *Narrow-Gap Lead Salts*, Springer, Berlin 1983.

[10] K. Lukoschus, S. Kraschinski, C. Nather, W. Bensch, R.K. Kremer, *J. Solid State Chem.* **177**, 951 (2004).

[11] T. Hashimoto, K. Hoya, M. Yamaguchi, I. Ichitsubo, *J. Phys. Soc. Jpn.* **31**, 679, (1971).

[12] J.H. Zhang, T.L.T. Birdwhistell, C.J. O'Connor, *Solid State Commun.* **74**, 443 (1990).

[13] J. Dijkstra, H.H. Weitering, C.F. van Bruggen, C. Haas, R.A. de Groot, *J. Phys. Condens. Matter* **1**, 9141 (1989).

[14] T. Hashimoto, M. Yamaguchi, *J. Phys. Soc. Jpn.* **27**, 1121 (1969).

[15] M. Akram, F.M. Nazar, *J. Mater. Sci.* **18**, 423 (1983).

[16] A. Begouen-Demeaux, G. Villers, P. Gibard, *J. Solid State Chem.* **15**, 178 (1975).

[17] L. Kilanski, M. Arciszewska, V. Domukhovski, W. Dobrowolski, V.E. Slynko, I.E. Slynko, *Acta Phys. Pol. A* **114**, 1145 (2008).

[18] L. Kilanski, M. Arciszewska, W. Dobrowolski, V. Domukhovski, V.E. Slynko, E.I. Slynko, *J. Appl. Phys.* **103**, 103901 (2009).

[19] L. Kilanski, R. Szymczak, W. Dobrowolski, K. Szałowski, V.E. Slynko, E.I. Slynko, *Phys. Rev. B* **82**, 094427 (2010).

[20] L. Kilanski, M. Górska, R. Szymczak, W. Dobrowolski, A. Podgórni, A. Avdonin, V. Domukhovski, V.E. Slynko, E.I. Slynko, *J. Appl. Phys.* **116**, 083904 (2014).